

# VECTOR CONCEPTS-BASED SPECTRAL MODELLING

Rastislav Lukac

Multimedia Laboratory, Dept. of ECE  
University of Toronto, 10 King's College Road  
Toronto, M5S 3G4, ON Canada  
e-mail: lukacr@ieee.org

Konstantinos N. Plataniotis

Multimedia Laboratory, Dept. of ECE  
University of Toronto, 10 King's College Road  
Toronto, M5S 3G4, ON Canada  
e-mail: kostas@dsp.utoronto.ca

## Abstract

*This paper presents a unique spectral modelling approach suitable for digital camera image processing. The proposed vector model combines both the magnitude and directional characteristics of the vectorial RGB color inputs and enforces orientation constraints in an orthogonal color system to produce outputs which can simultaneously match luminance and chrominance characteristics of the captured image. Thus, the model enhances the performance of commonly used practical demosaicking solutions. Moreover, spectral models previously used in demosaicking can be seen as special cases of the proposed vector model.*

**Keywords** — Color imaging; single-sensor digital cameras; spectral modelling; vector model.

## 1 Introduction

Single-sensor imaging devices, such as digital still and video cameras, image-enabled mobile phones and personal digital assistants, utilize a color filter array (CFA) in conjunction with a charge-coupled device (CCD) or a complementary metal oxide semiconductor (CMOS) sensor to capture the visual scene [1]. Due to the mosaic layout of color filters and the monochromatic nature of a single image sensor, the acquired CFA data constitutes a mosaic-like, gray-scale, image. The full-color information is recovered from the spatially adjacent CFA samples using demosaicking [1]-[5].

The powerful demosaicking procedures utilize both the spatial and spectral properties of the neighboring CFA samples in an attempt to eliminate color shifts in the demosaicked output. This is done by enforcing a spectral model during the demosaicking process. The most commonly used solutions are the color-difference model [6], the color-ratio model [7] and its normalized variants [8],[9]. Operating over spatially neighboring color pixels, the color-difference model is used to guarantee the minimization of the magnitude error, whereas the color-ratio model is based on the assumption of hue constancy in localized image regions. However, both modelling assumptions break down in high-frequency image regions (edges and fine details), where both magnitude and hue characteristics of the natural RGB image vary significantly. Although the normalized color-ratio models of [8],[9] can overcome this drawback by projecting the available components into their more uniform equivalents, similarly to the previous solutions they does not fully utilize the essential spectral characteristics of the inputs, thus introducing an estimation error.

This paper presents a powerful vector spectral model which overcomes the limitations of single-sensor imaging

devices and avoids the lacks of previous spectral models while generalizing these models as the special cases. Using the complete spectral information and both magnitude and directional characteristics of the color pixels, the proposed model estimates the color component under consideration by solving a quadratic equation which can be reduced to computationally-attractive processing solutions. It will be shown that the use of the proposed model in demosaicking avoids false color shifts and moire noise, increases sharpness of the demosaicked output and results in visually pleasing color images.

## 2 Vector Model

It is well-known that natural images consist of regions which exhibit similar, if not identical, directional properties [10]-[13]. Since the color-chromaticity relates to vectors' directional characteristics [10], two neighboring RGB vectors  $\mathbf{x}_{(p,q)} = [x_{(p,q)1}, x_{(p,q)2}, x_{(p,q)3}]$  and  $\mathbf{x}_{(i,j)} = [x_{(i,j)1}, x_{(i,j)2}, x_{(i,j)3}]$ , with  $x_{(\cdot,\cdot)k}$  denoting the R ( $k = 1$ ), G ( $k = 2$ ) and B ( $k = 3$ ) component, have the same chromaticity characteristics if they are considered to be collinear vectors in the RGB color space. The constraint can be expressed as  $\langle \mathbf{x}_{(p,q)}, \mathbf{x}_{(i,j)} \rangle = 0$  where  $\langle \cdot, \cdot \rangle$  denotes the angle between the two vectors.

Since this orientation constraint applies to any two vectorial entries it is also applicable to linearly shifted vectors [14]:

$$\langle \mathbf{x}_{(p,q)} + \gamma \mathbf{I}, \mathbf{x}_{(i,j)} + \gamma \mathbf{I} \rangle = 0 \quad (1)$$

where  $\mathbf{I}$  is a unit vector of proper dimension and  $\gamma$  is a linear shift applied, in a component-wise manner, to vector  $\mathbf{x}_{(\cdot,\cdot)}$  to produce its shifted variant  $\mathbf{x}'_{(\cdot,\cdot)} = \mathbf{x}_{(\cdot,\cdot)} + \gamma \mathbf{I}$ . For modelling purposes the process modifies both the orientation and magnitude characteristics of the input vectors  $\mathbf{x}_{(\cdot,\cdot)}$ .

### 2.1 Spectral Modelling Process

Modelling  $\mathbf{x}_{(p,q)}$  using  $\mathbf{x}_{(i,j)}$  under the constraint  $\langle \mathbf{x}_{(p,q)}, \mathbf{x}_{(i,j)} \rangle = 0$  in practice means that the modelled vector  $\mathbf{x}_{(p,q)}$  will share the same chromaticity line with  $\mathbf{x}_{(i,j)}$  in the vector space. If the original vectors  $\mathbf{x}_{(\cdot,\cdot)}$  occupy the same chromaticity line, then their linear shift results in  $\langle \mathbf{x}'_{(p,q)}, \mathbf{x}'_{(i,j)} \rangle = 0$  for  $\mathbf{x}_{(p,q)} = \mathbf{x}_{(i,j)}$  or  $\mathbf{x}_{(i,j)}$  denoting an achromatic color vector (i.e.  $x_{(i,j)k}$  is constant for  $k = 1, 2, 3$ ). However, for  $\mathbf{x}_{(p,q)} \neq \mathbf{x}_{(i,j)}$  with  $\mathbf{x}_{(i,j)}$  denoting a chromatic color vector the procedure results in  $\langle \mathbf{x}'_{(p,q)}, \mathbf{x}'_{(i,j)} \rangle \neq 0$ .

Linearly shifting  $\mathbf{x}_{(\cdot,\cdot)}$  leaves the component-wise magnitude differences  $\Delta_k = x_{(p,q)k} - x_{(i,j)k}$  unchanged. However, calculating the  $k$ -th color component in  $\mathbf{x}'_{(p,q)}$  under the constraint  $\langle \mathbf{x}'_{(p,q)}, \mathbf{x}'_{(i,j)} \rangle = 0$  normalizes the corresponding difference  $\Delta_k$  towards the differences calculated in other color channels. Thus, the procedure unifies the  $\Delta_k$  terms for  $\gamma \rightarrow \infty$ . Inverse shifting normalization via  $-\gamma$  does not affect the differences  $\Delta_k$  while attempting to restore the original orientation characteristics. The process results in  $\langle \mathbf{x}'_{(p,q)}, \mathbf{x}_{(p,q)} \rangle = \langle \mathbf{x}'_{(p,q)} - \gamma \mathbf{I}, \mathbf{x}_{(p,q)} \rangle$  for  $\mathbf{x}_{(p,q)} = \mathbf{x}_{(i,j)}$  and the achromatic color vector  $\mathbf{x}_{(i,j)}$ . For  $\mathbf{x}_{(p,q)} \neq \mathbf{x}_{(i,j)}$  with the chromatic color vector  $\mathbf{x}_{(i,j)}$  the modelling process results in  $\langle \mathbf{x}'_{(p,q)}, \mathbf{x}_{(p,q)} \rangle > \langle \mathbf{x}'_{(p,q)} - \gamma \mathbf{I}, \mathbf{x}_{(p,q)} \rangle$ . This suggests that the process forms the resultant vector  $\mathbf{x}'_{(p,q)} - \gamma \mathbf{I}$  closer, compared to the  $\gamma$ -shifted entry  $\mathbf{x}'_{(p,q)}$ , to the vector  $\mathbf{x}_{(p,q)}$  which can be obtained using only the directional information ( $\gamma = 0$ ). Thus, the proposed spectral model attempts to simultaneously preserve the orientation and magnitude characteristics of the color vectors in a localized image area while reducing modelling errors [14].

## 2.2 Cost-Effective Modelling Expressions

Using Cartesian representation, the orientation constraint of (1) can be re-written as follows:

$$\frac{\sum_{k=1}^3 (x_{(p,q)k} + \gamma)(x_{(i,j)k} + \gamma)}{\sqrt{\sum_{k=1}^3 (x_{(p,q)k} + \gamma)^2} \sqrt{\sum_{k=1}^3 (x_{(i,j)k} + \gamma)^2}} = 1 \quad (2)$$

The above expression can be equivalently re-arranged in the following form:

$$\frac{(x'_{(p,q)1}x'_{(i,j)2} - x'_{(p,q)2}x'_{(i,j)1})^2 + (x'_{(p,q)1}x'_{(i,j)3} - x'_{(p,q)3}x'_{(i,j)1})^2 + (x'_{(p,q)2}x'_{(i,j)3} - x'_{(p,q)3}x'_{(i,j)2})^2}{(x'_{(p,q)1}x'_{(i,j)2} - x'_{(p,q)2}x'_{(i,j)1})^2 + (x'_{(p,q)1}x'_{(i,j)3} - x'_{(p,q)3}x'_{(i,j)1})^2 + (x'_{(p,q)2}x'_{(i,j)3} - x'_{(p,q)3}x'_{(i,j)2})^2} = 0 \quad (3)$$

where  $x'_{(\cdot,\cdot)k} = x_{(\cdot,\cdot)k} + \gamma$  for  $k = 1, 2, 3$ .

Any component  $x_{(p,q)k} = x'_{(p,q)k} - \gamma$ , for  $k = 1, 2, 3$ , can be determined from (2) based on the three components of  $\mathbf{x}'_{(i,j)}$  and the two available components of  $\mathbf{x}'_{(p,q)}$  as the root  $y = (-b \pm \sqrt{b^2 - 4ac})/(2a)$  of the quadratic equation  $ay^2 + by + c = 0$  where  $y$  denotes the color component under consideration. It can be shown [14] that (2) leads to a unique solution defined as  $y = -b/(2a)$  due to zero discriminant  $b^2 - 4ac = 0$ , as derived based on (3). Thus, the modelling assumption of (2) with the shifted R component  $x'_{(p,q)1} = y$ , results in (4). Similarly, using the shifted G component  $x'_{(p,q)2} = y$  or B component  $x'_{(p,q)3} = y$  the modelling expression in (2) results in (5) and (6), respectively.

Note that the proposed spectral model can be used in support of vectors of an arbitrary dimensionality. If  $\mathbf{x}_{(\cdot,\cdot)}$  denotes two-component vectors defined in RG or BG vector representation, then the R component  $x_{(p,q)1}$  can be obtained via (2) as follows:

$$x_{(p,q)1} = -\gamma + \frac{(x_{(p,q)2} + \gamma)(x_{(i,j)1} + \gamma)}{x_{(i,j)2} + \gamma} \quad (7)$$

Since demosaicking solutions often calculate the G component  $x_{(p,q)2}$  using R or B components,  $x_{(p,q)2}$  can be obtained as follows:

$$x_{(p,q)2} = \begin{cases} -\gamma + \frac{(x_{(p,q)1} + \gamma)(x_{(i,j)2} + \gamma)}{x_{(i,j)1} + \gamma} & \text{or} \\ -\gamma + \frac{(x_{(p,q)3} + \gamma)(x_{(i,j)2} + \gamma)}{x_{(i,j)3} + \gamma} \end{cases} \quad (8)$$

Finally, the B component  $x_{(p,q)3}$  can be determined as follows:

$$x_{(p,q)3} = -\gamma + \frac{(x_{(p,q)2} + \gamma)(x_{(i,j)3} + \gamma)}{x_{(i,j)2} + \gamma} \quad (9)$$

## 2.3 Special Cases of the Vector Model

The refined vector concept and the ability to model spectral characteristics using different contributions of luminance and chrominance information make the proposed model a generalized solution for single-sensor imaging. Thus, the previous models used in demosaicking can be obtained as special cases of the vector model [14], as reported below.

By setting  $\gamma = 0$  in the two-component modelling expressions (7)-(9) the vector model reduces to the well-known color-ratio model [7]:

$$\frac{x_{(p,q)1}}{x_{(i,j)1}} = \frac{x_{(p,q)2}}{x_{(i,j)2}} \quad \text{or} \quad \frac{x_{(p,q)3}}{x_{(i,j)3}} = \frac{x_{(p,q)2}}{x_{(i,j)2}} \quad (10)$$

For a non-zero parameter  $\gamma$ , two-component equations (7)-(9) can be re-written to obtain normalized color-ratios [8],[9]:

$$\frac{x_{(p,q)1} + \gamma}{x_{(i,j)1} + \gamma} = \frac{x_{(p,q)2} + \gamma}{x_{(i,j)2} + \gamma} \quad \text{or} \quad \frac{x_{(p,q)3} + \gamma}{x_{(i,j)3} + \gamma} = \frac{x_{(p,q)2} + \gamma}{x_{(i,j)2} + \gamma} \quad (11)$$

For  $\gamma \rightarrow \infty$  in (7)-(9) the proposed model becomes equivalent to the color-difference model [6]:

$$\begin{aligned} x_{(p,q)1} - x_{(i,j)1} &= x_{(p,q)2} - x_{(i,j)2} \quad \text{or} \\ x_{(p,q)3} - x_{(i,j)3} &= x_{(p,q)2} - x_{(i,j)2} \end{aligned} \quad (12)$$

since the procedure normalizes the component-wise differences calculated using shifted components.

Finally, by setting  $\gamma = 0$  in three-component modelling expression (4)-(6) the proposed model is equivalent to the chrominance model [13]:

$$x_{(p,q)1} = \frac{x_{(p,q)2}x_{(i,j)1}x_{(i,j)2} + x_{(p,q)3}x_{(i,j)1}x_{(i,j)3}}{x_{(i,j)2}^2 + x_{(i,j)3}^2} \quad (13)$$

$$x_{(p,q)2} = \frac{x_{(p,q)1}x_{(i,j)1}x_{(i,j)2} + x_{(p,q)3}x_{(i,j)2}x_{(i,j)3}}{x_{(i,j)1}^2 + x_{(i,j)3}^2} \quad (14)$$

$$x_{(p,q)3} = \frac{x_{(p,q)1}x_{(i,j)1}x_{(i,j)3} + x_{(p,q)2}x_{(i,j)2}x_{(i,j)3}}{x_{(i,j)1}^2 + x_{(i,j)2}^2} \quad (15)$$

However, unlike the chrominance model, the proposed model produces outputs which can simultaneously match luminance and chrominance characteristics of the captured image, resulting in visually pleasing images.

$$x_{(p,q)1} = -\gamma + \frac{(x_{(p,q)2} + \gamma)(x_{(i,j)1} + \gamma)(x_{(i,j)2} + \gamma) + (x_{(p,q)3} + \gamma)(x_{(i,j)1} + \gamma)(x_{(i,j)3} + \gamma)}{(x_{(i,j)2} + \gamma)^2 + (x_{(i,j)3} + \gamma)^2} \quad (4)$$

$$x_{(p,q)2} = -\gamma + \frac{(x_{(p,q)1} + \gamma)(x_{(i,j)1} + \gamma)(x_{(i,j)2} + \gamma) + (x_{(p,q)3} + \gamma)(x_{(i,j)2} + \gamma)(x_{(i,j)3} + \gamma)}{(x_{(i,j)1} + \gamma)^2 + (x_{(i,j)3} + \gamma)^2} \quad (5)$$

$$x_{(p,q)3} = -\gamma + \frac{(x_{(p,q)1} + \gamma)(x_{(i,j)1} + \gamma)(x_{(i,j)3} + \gamma) + (x_{(p,q)2} + \gamma)(x_{(i,j)2} + \gamma)(x_{(i,j)3} + \gamma)}{(x_{(i,j)1} + \gamma)^2 + (x_{(i,j)2} + \gamma)^2} \quad (6)$$

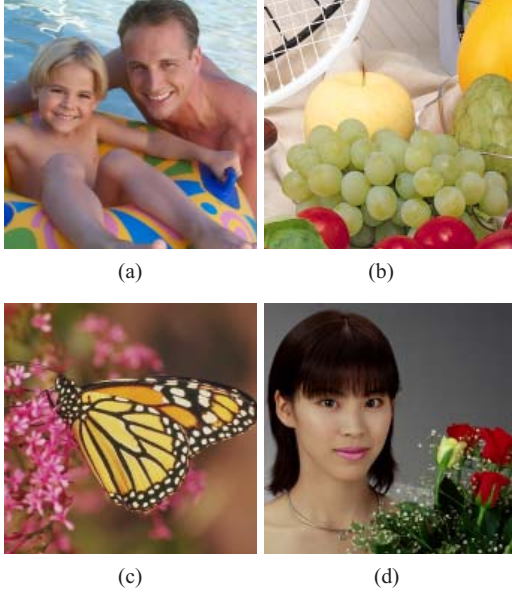


**Figure 1.** Test color images with  $512 \times 512$  spatial resolution: (a) Water, (b) Fruits, (c) Butterfly, (d) Woman.

### 3 Experimental Results

A number of test images, such as those shown in *Fig. 1*, have been utilized to determine the performance the proposed vector model. To obtain a CFA image, original images were samples using the well-known Bayer CFA [1] with the GRGR phase in the first row. The images were demosaicked using a four-step demosaicking procedure based on the data-adaptive processing concept of [5], the simple edge-sensing mechanism of [15] and the proposed spectral model in (1). In the first demosaicking step, the G components are demosaicked using the two-component modelling expression in (8). In the second step, two-component expressions in (7) and (9) are used to demosaick the R and B components, respectively. Since this step completely restores color information, three-component expressions are employed in the two remaining steps to re-evaluate the demosaicked components. After the G components are re-evaluated using (5), the demosaicking procedure completes with (4) and (6) by re-generating the demosaicked R and B components. Details on the proposed demosaicking solution can be found in [14].

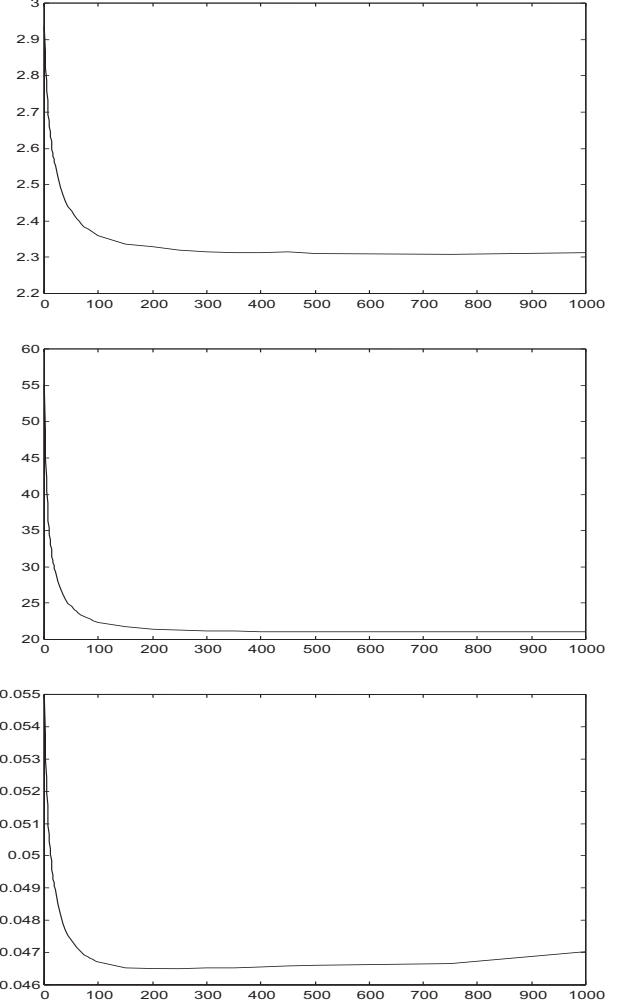


**Figure 2.** Error criteria vs. parameter  $\gamma \in \langle 0, 1000 \rangle$ : (top) MAE, (middle) MSE, (bottom) NCD.

Performance was measured by comparing the original full color images to the demosaicked images. To facilitate the objective comparisons [2], the RGB color space based mean absolute error (MAE) and mean square error (MSE) criteria, the CIE-LUV color space based normalized color difference (NCD) criterion are used to objectively measure the difference between the original color image and the demosaicked image.

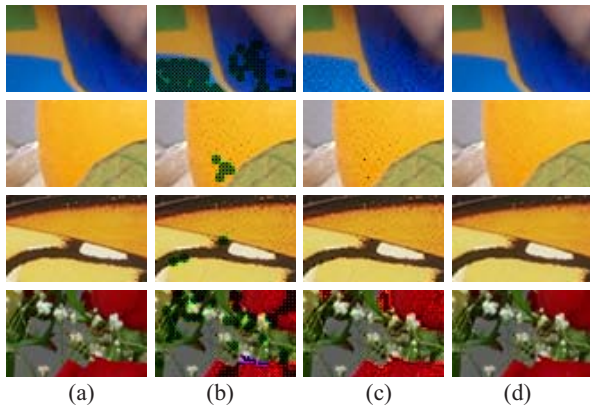


**Figure 3.** Achieved results: (a) original images, (b)  $\gamma = 0$ , (c)  $\gamma = 1$ , (d)  $\gamma = 256$ .

Fig.2 shows the performance of the proposed framework depending on the parameter  $\gamma$ . The results were averaged over four images shown in Fig.1. The performance of the proposed framework mainly increases as  $\gamma \rightarrow 200$ , with consistently good results obtained for  $\gamma = 250$ . Expansion of  $\gamma$  beyond the value 700 was found rather counter-productive, especially in terms of NCD. Therefore, we propose the use of  $\gamma = 256$  in practice. Such a setting will keep the shifted components in a range represented by nine bits.

Fig.3 shows enlarged parts of the images cropped in areas with high edge density. As it can be seen, the use of the recommended setting ( $\gamma = 256$ ) in our framework results in the enhanced visual quality of the demosaicked image. In this case, the proposed solution produces a demosaicked output with an excellent fidelity in both color and structure.

## 4 Conclusions

A vector spectral model for single-sensor and color imaging was introduced. The model simultaneously utilizes both the directional and the magnitude characteristics of the neighboring color vectors. Moreover, it generalizes spectral models which are routinely used in demosaicking solutions. Experimental results showed that demosaicking based on the proposed vector model preserves natural coloration and sharpness of the demosaicked images.

## References

- [1] R. Lukac and K. N. Plataniotis, "Color filter arrays: Design and performance analysis," *IEEE Transactions on Consumer Electronics*, vol. 51, no. 4, pp. 1260-1267, November 2005.
- [2] R. Lukac, K. N. Plataniotis, and D. Hatzinakos, "Color image zooming on the Bayer pattern," *IEEE Transactions on Circuit and Systems for Video Technology*, vol. 15, no. 11, pp. 1475-1492, November 2005.
- [3] L. Zhang and X. Wu, "Color demosaicking via directional linear minimum mean square-error interpolation," *IEEE Transactions on Image Processing*, vol. 14, no. 12, pp. 2167-2178, December 2005.
- [4] B. K. Gunturk, J. Glotzbach, Y. Altunbasak, R. W. Schaffer, and R. M. Merserau, "Demosaicking: Color filter array interpolation," *IEEE Signal Processing Magazine*, vol. 22, no. 1, pp. 44-54, January 2005.
- [5] R. Lukac and K. N. Plataniotis, "Data-adaptive filters for demosaicking: A framework," *IEEE Transactions on Consumer Electronics*, vol. 51, no. 2, pp. 560-570, May 2005.
- [6] J. Adams, "Design of practical color filter array interpolation algorithms for digital cameras," *Proceedings of the SPIE*, vol. 3028, pp. 117-125, February 1997.
- [7] D. R. Cok, "Signal processing method and apparatus for producing interpolated chrominance values in a sampled color image signal," *U.S. Patent 4 642 678*, February 1987.
- [8] R. Lukac, K. Martin, and K. N. Plataniotis, "Demosaicked image postprocessing using local color ratios," *IEEE Transactions on Circuit and Systems for Video Technology*, vol. 14, no. 6, pp. 914-920, June 2004.
- [9] R. Lukac and K. N. Plataniotis, "Normalized color-ratio modeling for CFA interpolation," *IEEE Transactions on Consumer Electronics*, vol. 50, no. 2, pp. 737-745, May 2004.
- [10] P. E. Trahanias, D. Karakos, and A. N. Venetsanopoulos, "Directional processing of color images: theory and experimental results," *IEEE Transactions on Image Processing*, vol. 5, no. 6, pp. 868-881, June 1996.
- [11] B. Tang, G. Sapiro, and V. Caselles, "Color image enhancement via chromaticity diffusion," *IEEE Transactions on Image Processing*, vol. 10, no. 5, pp. 701-707, May 2001.
- [12] R. Lukac, B. Smolka, K. Martin, K. N. Plataniotis, and A. N. Venetsanopoulos, "Vector filtering for color imaging," *IEEE Signal Processing Magazine*, vol. 22, no. 1, pp. 74-86, January 2005.
- [13] D. Keren and M. Osadchy, "Restoring subsampled color images," *Machine Graphics and Vision*, vol. 11, no. 4, pp. 197-202, December 1999.
- [14] R. Lukac and K. N. Plataniotis, "A vector spectral model for digital camera image processing," *IEEE Transactions on Circuit and Systems for Video Technology*, submitted.
- [15] L. Chang and Y. P. Tang, "Effective use of spatial and spectral correlations for color filter array demosaicking," *IEEE Transactions on Consumer Electronics*, vol. 50, no. 2, pp. 355-365, May 2004.